THEORETICA CHIMICA ACTA

Theoret. Chim. Acta (Berl.) 61, 473–484 (1982)

A Concise Representation of Adsorbate-Surface Interactions. II. An Application to Pt(111)+CO, W(110)+CO and Pt(112)+CO Systems

Hisayoshi Kobayashi and Masaru Yamaguchi

Faculty of Living Science, Kyoto Prefectural University, Kyoto, Japan

Satohiro Yoshida

Faculty of Engineering, Kyoto University, Kyoto, Japan

A method is presented to represent the chemisorptive interactions concisely. The canonical molecular orbitals of a chemisorption system are transformed into new orbitals where the charge transfer interactions between the surface and the adsorbate are maximized or minimized. The chemisorptive bonds are well described by a small number of the transformed orbitals. The analysis of chemisorptive interactions is carried out for the Pt(111)+CO, W(110)+CO and Pt(112)+CO systems. The weakening of the C—O bond in the W(110) face and in the trench region of the Pt(112) face is larger than that in the Pt(111) face in conformity with the experimental data. The interactions are, to a good approximation, represented by five or six orbitals and are explained in terms of the σ and π donation of CO to the surface and the π back donation to CO.

Key words: Chemisorption – MO calculation – Localized orbital.

1. Introduction

In chemical reactions, new chemical bonds are formed through the approach of two molecules (referred to as subsystems in a reaction system) and the interaction between them. The changes in bonds are described by molecular orbitals (MOs) of the system. With increase in size of the system, the number of MOs increases, and the individual MO contributes to the bond formation only to a very limited extent. Furthermore, usual canonical MOs spread out over the whole system.

0040-5744/82/0061/0473$02.40

So they are not convenient to describe the orbital interactions responsible for fission and formation of bonds. In a previous article, we presented a method to obtain a new set of orbitals from canonical MOs by unitary transformation [1]. The interactions between subsystems are maximized or minimized in the new orbitals, which are referred to as the interaction localized orbitals (ILOs). The modes of orbital interaction are clearly visualized in terms of a few ILOs corresponding to the maximized interaction.

In this article, the method is applied to the adsorption of CO on the Pt(111), W(110) and Pt(112) surfaces. Definite differences have been reported between the two metals. CO is adsorbed associatively on Pt(111) [2], but the fission of C—O bond occurs on W(110) [2–5]. Further, in the adsorption on stepped surfaces, new adsorbed states which do not exist on the flat (111) surface, appear [6–8]. We will discuss the changes in interactions due to the difference in metal atoms for the Pt(111)+CO and W(110)+CO systems, and due to the difference in two adsorption sites for the Pt(112)+CO system.

2. Method

The method to obtain the ILO is described in our previous article [1]. In the present article, the method is somewhat modified in order to localize only the net interactions contributing to the changes in bonds, and thus it is presented again. The MOs ψ of the system are expressed in terms of the MOs ϕ of the subsystems, A and B, as Eq. (1).

$$\psi_i = \sum_p^A \phi_p T_{pi} + \sum_q^B \phi_q T_{qi}, \tag{1}$$

where T is a matrix composed of the expansion coefficients. Let Ω be the operator describing the interactions between the subsystems, and then the contribution to the interaction from the MO ψ_i is given by the expectation value in Eq. (2).

$$\langle \psi_i | \Omega | \psi_i \rangle, \tag{2}$$

where the bra and ket notation implies the integration over the space. The ILO, ρ is determined so that the expectation value of Ω, Eq. (3) should have an extremum.

$$\lambda = \langle \rho | \Omega | \rho \rangle / \langle \rho | \rho \rangle. \tag{3}$$

The ρ is represented as a linear combination of the occupied ψ as Eq. (4).

$$\rho_l = \sum_i^{\text{occ}} \psi_i U_{il}, \tag{4}$$

where U is a unitary matrix for the transformation. Substituting Eq. (4) into Eq. (3) and equating the variation with respect to U_{il} to zero, we obtain a system of linear equations which is analogous to the secular equation in the usual MO theories, as Eq. (5).

$$\sum_j (\langle \psi_i | \Omega | \psi_j \rangle - \delta_{ij} \lambda) U_{jl} = 0. \tag{5}$$

As the explicit form of Ω, the off-diagonal elements in the Fock matrix, which has determined the ψ, are employed with a projection operator. This seems to be a simple and reasonable choice since the Fock matrix represents the field felt by one electron, while other choice for Ω also may be possible. For convenience in the representation of Ω, the Fock matrix is written in terms of the ϕ in Eq. (6).

$$\Omega = \left(\sum_{p}^{A-o} \sum_{q}^{B-v} + \sum_{p}^{A-v} \sum_{q}^{B-o} \right) (|\phi_p\rangle F_{pq} \langle \phi_q| + |\phi_q\rangle F_{qp} \langle \phi_p|), \tag{6}$$

where "$A-o$" and "$B-v$" mean the occupied MOs in the subsystem A and the vacant MOs in the subsystem B, respectively, and "$A-v$" and "$B-o$" have similar meaning. Eq. (6) reveals that the Ω includes only the charge transfer (CT) interactions between subsystems. This is the modified point in the present work, and it is reasonable since the CT interactions are exclusively responsible for the bond formation between subsystems and the interactions could explain most of the bond weakening within a subsystem. The matrix element for Ω is evaluated by multiplying both sides of Eq. (6) by Eq. (1) and by integrating over space, as Eq. (7).

$$\langle \psi_i | \Omega | \psi_j \rangle = \left(\sum_{p}^{A-o} \sum_{q}^{B-v} + \sum_{p}^{A-v} \sum_{q}^{B-o} \right) (T_{pi} T_{qj} + T_{pj} T_{qi}) F_{pq}, \tag{7}$$

where the overlap integral resulting between the different subsystems, $\langle \phi_p | \phi_q \rangle$ is neglected from chemical insight.

The eigenvalue λ and eigenvector U are obtained by diagonalization of the symmetry matrix whose elements are represented by Eq. (7). The λ indicates the strength of (CT) interaction in the ILO and the bonding ($\lambda < 0$) or antibonding ($\lambda > 0$) character of the interaction. In general the individual ILO represents two CT interactions, that is, the CT interaction from the subsystem A to B, and the reverse CT interaction. The λ could also be separated into the two parts, $\lambda^{A \to B}$ and $\lambda^{B \to A}$, as Eq. (8).

$$\begin{aligned} \lambda_l &= 2 \sum_{p}^{A-o} \sum_{q}^{B-v} V_{pl} V_{ql} \langle \phi_p | \Omega | \phi_q \rangle + 2 \sum_{p}^{A-v} \sum_{q}^{B-o} V_{pl} V_{ql} \langle \phi_p | \Omega | \phi_q \rangle \\ &= \lambda_l^{A \to B} + \lambda_l^{B \to A} \end{aligned} \tag{8}$$

where

$$V_{pl} = \sum_{i}^{\text{occ}} T_{pi} U_{il}. \tag{9}$$

The mode of each CT interaction in the ILO is clearly visualized by illustrating the coefficients, V_{pl} responsible for that interaction rather than all the coefficients composing the ρ_l. Let D be the expansion coefficient matrix of the ϕ by the atomic orbital (χ), and then ρ is expressed as Eq. (10).

$$\begin{aligned} \rho_l &= \sum_r \sum_p \chi_r D_{rp} V_{pl} \\ &= \left(\sum_{r}^{A} \sum_{p}^{A-o} + \sum_{r}^{B} \sum_{p}^{B-v} \right) \chi_r D_{rp} V_{pl} + \left(\sum_{r}^{A} \sum_{p}^{A-v} + \sum_{r}^{B} \sum_{p}^{B-o} \right) \chi_r D_{rp} V_{pl}. \end{aligned} \tag{10}$$

New coefficient matrices, $R^{A\to B}$ and $R^{B\to A}$ are defined in Eq. (11).

$$R_{rl}^{A\to B} = \left(\sum_{p}^{A-o} + \sum_{p}^{B-v} \right) D_{rp} V_{pl},$$
$$R_{rl}^{B\to A} = \left(\sum_{p}^{A-v} + \sum_{p}^{B-o} \right) D_{rp} V_{pl}. \tag{11}$$

$R_{rl}^{A\to B}$ and $R_{rl}^{B\to A}$ represent the AO coefficients which are responsible for the CT interaction from the subsystem A to B and that from the subsystem B to A, respectively, in the ρ_l.

Description of Chemisorption Systems and Calculation Method

Surfaces are represented by one or two layer slab models. We consider a molecular unit cell (MUC) as a unit of the periodicity parallel to the surface or parallel to the macroscopic plane of the stepped surface. The MUCs contain eight metal atoms in the first and second layers for the Pt(111) and W(110) surfaces, and the MUC for the Pt(112) surface consists of nine atoms in the first layer. These MUCs are illustrated in Fig. 1 with adsorption sites of CO. The adsorbed CO has a bridged configuration. For the stepped Pt(112) surface, two adsorption sites are examined, and they are tentatively referred to as the terrace and bottom sites. The latter is in the trench region of the stepped structure. The C—O bond length was fixed to 1.15 Å in all the sites, since it is invariant over the transition metal carbonyl complexes within 0.02 Å [9–11]. The value of 2.0 Å was adopted for the nearest W—C and Pt—C bond lengths by reference to the W—C bond length measured in the corresponding carbonyl complex and to the Pt—C bond length estimated in the other MO calculation [10–12].

Two dimensional repetition of the MUC describes the whole surface and the ordered array of adsorbate. The eigenfunctions of the system are referred to as the Bloch molecular orbitals (BMOs) since they extend repeatedly beyond MUCs like the Bloch functions and are dealt with as usual MOs within each MUC. The CNDO/2 approximation is employed to obtain the BMOs. The parameters for Pt and W atoms are estimated by the authors, and they are shown in Table 1. For C and O atoms, the standard values by Pople and co-workers are used [13].

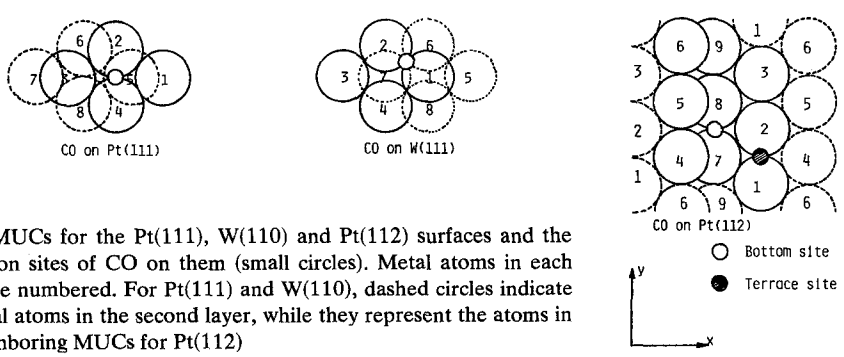

Fig. 1. MUCs for the Pt(111), W(110) and Pt(112) surfaces and the adsorption sites of CO on them (small circles). Metal atoms in each MUC are numbered. For Pt(111) and W(110), dashed circles indicate the metal atoms in the second layer, while they represent the atoms in the neighboring MUCs for Pt(112)

Table 1. Parameters for Pt and W atoms

	$\zeta_{s,p}$	ζ_d	$1/2(I+A)_s$	$1/2(I+A)_p$	$1/2(I+A)_d$	$-\beta_{s,p}$	$-\beta_d$
Pt	1.79[a]	2.31[b]	4.5	1.5	15.0	6.0	10.0
W	1.64[a]	1.75[b]	3.0	1.0	6.0	4.5	6.0

[a] See Ref. [14].
[b] See Ref. [15].

4. Results and discussion

Table 2 shows several λ values, that is, eigenvalues of ILOs in increasing order for the four chemisorption systems. The λ is a measure of the adsorbate-surface interactions in the ILO, and large negative λ means the strong bonding interaction. The ILO-1 shows the dominant bonding interaction over the other ILOs for the four systems. The λ increases with the number of ILO and it rapidly approaches to zero in the ILO-8 or -9. In the Pt(111)+CO and Pt(112)+CO systems, the second jump of λ is seen between the ILOs-5 and -6. The sum of the first five λ values becomes more than 94% of the sum of all the negative values of λ. In other words, more than 94% of the bonding interactions is represented by the five ILOs. In the W(110)+CO system, the second jump of λ appears between the ILOs-6 and -7. The first six ILOs explain almost all the bonding interactions (more than 99%). Thus, in the qualitative and semiquantitative discussion of the interactions, it will be sufficient to discuss the first five ILOs for the Pt(111)+CO and Pt(112)+CO systems, and the first six ILOs for the W(110)+CO system. We could say that the adsorbate-surface interactions are effectively represented in terms of the ILO although there are forty-five, twenty-nine and fifty occupied BMOs in the Pt(111)+CO, W(110)+CO and Pt(112)+CO systems, respectively.

Table 2. Leading nine eigenvalues, λ (eV) for the four chemisorption systems

			Pt(112)+CO	
	Pt(111)+CO	W(110)+CO	Terrace site	Bottom site
l	λ_l	λ_l	λ_l	λ_l
1	−9.17	−14.62	−9.97	−14.55
2	−3.19	−8.98	−3.35	−8.05
3	−2.56	−5.22	−2.69	−5.12
4	−1.88	−2.91	−2.46	−4.20
5	−1.60	−1.89	−2.21	−3.78
6	−0.59	−1.70	−0.92	−1.23
7	−0.23	−0.36	−0.26	−0.79
8	−0.02	−0.01	−0.06	−0.22
9	−0.00	−0.00	−0.00	−0.00

Table 3. Some $\lambda^{CO\to Pt}$ and $\lambda^{Pt\to CO}$ values (eV) for the four chemisorption systems[a]

	Pt(111)+CO		W(110)+CO		Pt(112)+CO Terrace		Pt(112)+CO Bottom	
l	$\lambda_l^{CO\to Pt}$	$\lambda_l^{PT\to CO}$	$\lambda_l^{CO\to W}$	$\lambda_l^{W\to CO}$	$\lambda_l^{CO\to Pt}$	$\lambda_l^{Pt\to CO}$	$\lambda_l^{CO\to Pt}$	$\lambda_l^{Pt\to CO}$
1	<u>−9.17</u>	−0.00	<u>−14.62</u>	0.00	<u>−9.93</u>	−0.04	<u>−14.53</u>	−0.02
2	−0.30	<u>−2.89</u>	−0.33	<u>−8.65</u>	<u>−3.14</u>	−0.21	<u>−7.99</u>	−0.06
3	−0.45	<u>−2.11</u>	<u>−4.75</u>	−0.47	−0.25	<u>−2.44</u>	−1.23	<u>−3.89</u>
4	<u>−1.59</u>	−0.29	<u>−2.61</u>	−0.30	−0.21	<u>−2.25</u>	<u>−3.23</u>	−0.97
5	<u>−1.55</u>	−0.05	−0.26	<u>−1.63</u>	<u>−1.96</u>	−0.25	−0.08	<u>−3.70</u>
6			<u>−1.69</u>	−0.01				

[a] Underlined values indicate the larger part of two CT interactions.

The ILOs generally contain both CT interactions; CT from CO to the surface and CT from the surface to CO. Each λ is separated into two parts, $\lambda^{CO\to M}$ and $\lambda^{M\to CO}$ (M = Pt or W) corresponding to the two CT interactions. Table 3 shows $\lambda^{CO\to M}$ and $\lambda^{M\to CO}$ for the first five or six ILOs in Table 2. The larger part in each λ is underlined, and is at least three times larger than the smaller part. So, separation of the two CT interactions seems to be satisfactory for characterization of the ILO by the larger CT interaction. The ILO-1 represents almost only the electron donation from CO to the surface for the four systems. In the other ILOs, relative magnitude and nature of individual interactions depend on the metal atoms and the adsorption sites of CO. Two ILOs mainly represent the CT interaction from the surface to CO, and two or three ILOs except for the ILO-1 mainly represent the reverse CT interaction.

Table 4 shows the leading elements of the $R^{CO\to Pt}$ or $R^{Pt\to CO}$ matrix defined in Eq. (11) for the ILOs-1 to -5 in the Pt(111)+CO system. Some of AO com-

Table 4. Leading $R^{CO\to Pt}$ or $R^{Pt\to CO}$ matrix elements for the ILOs-1 to -5 in the Pt(111)+CO system[a]

ILO-1 $R^{CO\to Pt}$		ILO-2 $R^{Pt\to CO}$		ILO-3 $R^{Pt\to CO}$		ILO-4 $R^{CO\to Pt}$		ILO-5 $R^{CO\to Pt}$	
(2)y	−0.138	(2)z^2	0.391	(1)xz	0.240	(1)x	−0.055	(2)s	−0.064
(2)z	0.120	(2)yz	−0.462	(1)x^2-y^2	−0.160	(2)x	0.054	(2)z	−0.077
(4)y	0.138	(4)z^2	−0.391	(2)xz	−0.383	(3)x	−0.056	(4)s	0.064
(4)z	0.120	(4)yz	−0.462	(2)xy	0.344	(4)x	0.054	(4)z	0.077
(C)s	0.827	(C)y	0.204	(3)xz	0.225	(C)x	0.468	(C)y	−0.491
(C)z	−0.264	(O)y	−0.133	(3)x^2-y^2	0.154	(O)x	0.722	(O)y	−0.757
(O)s	0.215			(4)xz	−0.383				
(O)z	−0.118			(4)xy	−0.344				
				(C)x	−0.149				
				(O)x	0.097				

[a] The atom to which the AO belong is indicated in the parenthesis. The number in the parenthesis corresponds to the number of metal atom shown in Fig. 1. The p_x, p_y and p_z AOs are abbreviated as x, y and z and so are the d AOs.

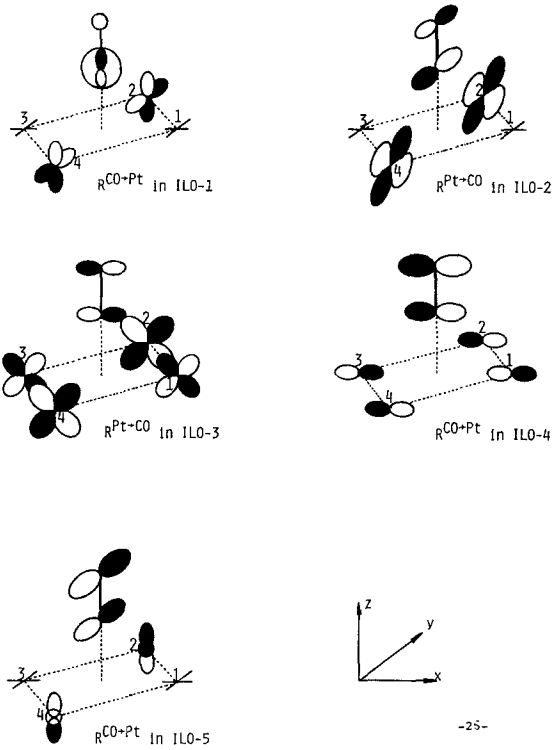

Fig. 2. Schematic illustration for the modes of the larger CT interaction represented by the ILOs-1 to -5 in the Pt(111) + CO system. For the numbers on the Pt atoms, refer to Fig. 1.

ponents in Table 4 are illustrated in Fig. 2 to visualize the modes of orbital interaction. The orbital pattern represented by the $R^{CO\to Pt}$ matrix for the ILO-1 shows a large orbital lobe on the C atom toward the surface. This type of interaction is known as the σ donation of CO. The orbital pattern in the CO moiety is, however, not the same as the 5σ orbital in free CO, and is composed of the 3σ, 4σ and 5σ orbitals as illustrated in Fig. 3. This rehybridization increases the component of the $2s$ AO rather than the $2p_z$ AO on the C atom, and it seems to be favorable for the bond formation at the bridged configuration. For the AOs on the surface, the $6p_y$ and $6p_z$ AOs on the Pt(2) and (4) atoms accept electrons from CO. The orbital patterns represented by the $R^{Pt\to CO}$ matrix for the ILOs-2 and -3 indicate the CT interaction from the surface to CO. The Pt $5d$ AOs donate electrons to CO, in which the orbital patterns are essentially

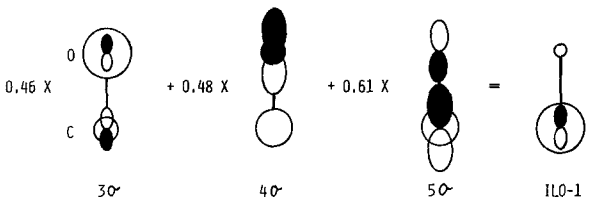

Fig. 3. Construction of the ILO-1 from the canonical BMOs on CO in the Pt(111) + CO system

the $2\pi(\pi^*)$ orbitals. The interaction is also known as the π back donation. The $R^{CO\to Pt}$ matrix for the ILOs-4 and -5 represents again the CT interaction from CO to the surface. The Pt 6s and 6p AOs accept electrons from the $1\pi(\pi)$ orbitals. The interaction could be suitably called as the π donation. The interactions by the σ and one of π orbitals (referred to as π_x orbital in the coordinate system in Fig. 2) on CO strictly mix each other through the interaction with the Pt atoms in the second layer. The mixing is, however, so small that the terms of "σ" and "π" could be used to characterize the interactions. Most of interactions occurs with the Pt atoms in the first layer, and this result does not suggest that the one layer model for the stepped (112) surface is an unrealistic approximation.

In the W(110)+CO system, we will first investigate the interactions represented by the ILOs-1 to -3 in detail, since the $\lambda^{CO\to W}$ or $\lambda^{W\to CO}$ values in these ILOs indicate much stronger interactions than those in the ILOs-4 to -6. The leading elements of the $R^{CO\to W}$ and $R^{W\to CO}$ matrices are shown in Table 5 for the ILOs-1 and -3 and for the ILO-2, respectively. The $R^{CO\to W}$ matrix for the ILO-1 shows again that the interaction is the σ donation from CO. The 6*s* AOs on the second layer W atoms (W(6) and (7)) considerably participate in this interaction. The W $5d_{xz}$ AOs as well as the 6*s* and 6*p* AOs accept electrons from CO since the *d* band is filled nearly half in W. The major part of the ILO-2 represents the π back donation from the W 5*d* AOs to the 2π orbital on CO. The major part of the ILO-3 represents the π donation from the 1π orbital to the $5d_{z^2}$

Table 5. Leading $R^{CO\to W}$ or $R^{W\to CO}$ matrix elements for the ILOs-1 to -3 in the W(110)+CO system[a]

ILO-1 $R^{CO\to W}$		ILO-2 $R^{W\to CO}$		ILO-3 $R^{CO\to W}$	
(1)*s*	−0.123	(1)z^2	−0.103	(1)z^2	0.144
(1)*y*	−0.121	(1)*xz*	−0.129	(2)z^2	−0.144
(1)*xz*	0.217	(1)*yz*	−0.339	(*C*)*x*	0.255
(2)*s*	−0.123	(1)x^2-y^2	0.186	(*C*)*y*	−0.421
(2)*y*	0.121	(2)z^2	0.103	(*O*)*x*	0.393
(2)*xz*	−0.217	(2)*xz*	−0.129	(*O*)*y*	−0.649
(6)*s*	0.109	(2)*yz*	−0.339		
(7)*s*	0.109	(2)x^2-y^2	−0.186		
(*C*)*s*	−0.771	(3)z^2	−0.124		
(*C*)*z*	0.238	(3)*yz*	0.227		
(*O*)*s*	−0.197	(3)x^2-y^2	0.116		
(*O*)*z*	0.123	(4)z^2	0.124		
		(4)*yz*	0.227		
		(4)x^2-y^2	−0.116		
		(*C*)*x*	−0.295		
		(*C*)*y*	−0.344		
		(*O*)*x*	0.191		
		(*O*)*y*	0.223		

[a] See caption of Table 4.

AOs on the W(1) and (2) atoms. Thus, the interactions represented by the ILOs-1 to -3 are explained in terms of the σ donation, π back donation and π donation, respectively. For the ILOs-4 to -6 representing the weaker interactions, the nature of the orbital patterns will be mentioned without tabulating the $R^{CO\to W}$ and $R^{W\to CO}$ matrices. The ILO-4 and -5 represent the π donation and π back donation, respectively. The ILO-6 contributes to the σ donation to some degree, but the AOs on CO constitute the C—O bond with the larger AO components on the O atom. Thus, the ILOs-2 and -5 represent the π back donation and the ILOs-3 and -4 represent the π donation in the W(110)+CO system. The difference between $\lambda_2^{W\to CO}$ and $\lambda_5^{W\to CO}$ is much larger than the corresponding differences in the Pt(111)+CO system, that is, the difference between the $\lambda_2^{Pt\to CO}$ and $\lambda_3^{Pt\to CO}$. The same trend is observed for the π donation. The difference between the $\lambda_3^{CO\to W}$ and $\lambda_4^{CO\to W}$ is larger than that between the $\lambda_4^{CO\to Pt}$ and $\lambda_5^{CO\to Pt}$. These results suggest that the asymmetry in the interactions through the two 1π orbitals or the two 2π orbitals is larger in the W(110) surface, which is probably ascribed to the difference in the electron configuration for the free surface rather than the difference in the crystal structure.

In the Pt(112) surface, the interactions through the σ and π_x orbitals on CO mix each other due to the stepped structure. In the terrace site, this mixing is as small as the mixing in the Pt(111) surface, but it is much larger in the bottom site. The interactions through the π_y orbitals are still independent of the interactions through the σ and π_x orbitals. The leading elements of the $R^{CO\to Pt}$ matrix are shown in Table 6 for the ILOs-1 and -2 at the terrace and bottom sites. The ILO-1 represents the σ donation from CO. The orbital pattern in the CO moiety is very similar to that in the ILO-1 for the Pt(111)+CO system, while the orbital

Table 6. Leading $R^{CO\to Pt}$ matrix elements for the ILOs-1 and -2 in the terrace and bottom sites for the Pt(112)+CO system[a]

ILO-1 (Terrace) $R^{CO\to Pt}$		ILO-2 (Terrace) $R^{CO\to Pt}$		ILO-1 (Bottom) $R^{CO\to Pt}$		ILO-2 (Bottom) $R^{CO\to Pt}$	
(1)y	0.191	(1)x	0.101	(2)xz	0.179	(2)s	0.091
(2)y	−0.191	(2)x	0.101	(2)x^2-y^2	−0.271	(2)x	−0.107
(3)xz	−0.167	(4)x	−0.118	(4)x	0.142	(4)y	−0.088
(3)x^2-y^2	0.268	(7)x	−0.104	(4)y	0.109	(5)y	0.088
(4)xz	0.111	(C)x	0.497	(5)x	0.142	(7)x	0.082
(4)x^2-y^2	−0.133	(O)x	0.767	(5)y	−0.109	(7)y	0.087
(7)s	0.119			(6)s	−0.103	(8)x	0.082
(7)xz	0.112			(7)y	0.133	(8)y	−0.087
(7)x^2-y^2	−0.122			(8)y	−0.133	(C)s	0.227
(C)s	0.652			(9)x^2-y^2	0.121	(C)x	0.332
(C)z	−0.188			(C)s	0.659	(C)z	−0.338
(O)s	0.175			(C)z	−0.134	(O)s	−0.444
(O)z	−0.116			(O)s	0.302	(O)x	0.512
				(O)x	−0.119		

[a] See caption of Table 4.

pattern in the surface region is not. In the terrace site, more surface AOs participate in the interaction, and the distinction between the roles of the Pt 5d AOs and 6s and 6p AOs is less definite. These differences may be ascribed to the change in the electronic state by the stepped structure even at the terrace site. The detailed discussion on the differences, however, could not be carried out since the number of surface layers and the surface area are different in the two MUCs for the Pt(111) and Pt(112) surfaces.

A remarkable characteristic on the terrace site is the enhancement of the π donation represented by the ILO-2. The corresponding ILO in the Pt(111)+CO system is the ILO-4. Comparing the $R^{CO\to Pt}$ matrices for the ILO-2 in Table 6 and for the ILO-4 in Table 4, we easily recognize that the coefficients for the Pt $6p_x$ AOs are approximately doubled in the terrace site while the coefficients for the $2p_x$ AOs on CO are nearly the same in the two systems. This result is consistent with the enhancement of the interaction. The ILOs-3 to -5 represent similar interactions with the ILOs-2, -3 and -5, respectively, in the Pt(111)+CO system, and they are not discussed further.

The differences in the interactions between the terrace and bottom sites are discussed. The electron donation represented by the ILOs-1 and -2 is greatly increased in the bottom site. The orbital patterns for these interactions are illustrated in Fig. 4. The CO moiety of the ILOs-1 and -2 is composed of the $2s$, $2p_z$ and also $2p_x$ AOs, and this result suggests that the mixing between the σ and $1\pi_x$ orbitals is remarkably large at the bottom site. These orbitals are rehybridized so that CO favorably interacts with both the bottom atoms (Pt(7) and (8)) and the top atoms (Pt(4) and (5)) of the stepped structure. The interactions of CO with the top atoms dominantly contribute to the Pt—O bond formation. These multicenter interactions also occur in the other ILOs, and they are responsible for the increased C—O bond weakening as well as the strong CO-surface interactions at the bottom site of the stepped surface. In Fig. 4, the AO components on the C atom are bonding with those on the Pt(2) atom in the ILO-2, while the interaction is antibonding in the ILO-1. In Table 6, the $R^{CO\to Pt}$ matrix for the ILO-1 shows considerable AO components on the Pt(3) atom for the terrace site and on the Pt(6) and (9) atoms for the bottom site. These AOs do not seem to interact strongly with the AOs on CO, since the distance between them is more than 4 Å. So it seems that these AO components

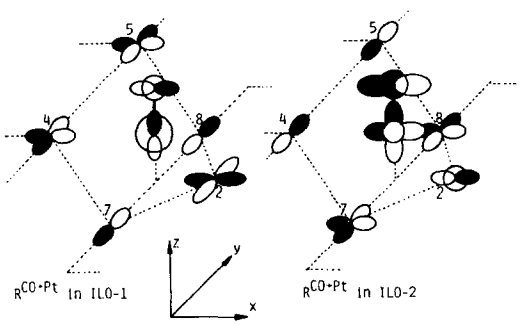

Fig. 4. Schematic illustration for the modes of the larger CT interaction represented by the ILOs-1 and -2 at the bottom site in the Pt(112)+CO system. For the numbers on the Pt atoms, refer to Fig. 1

on the Pt atoms have appeared due to the boundary conditions imposed on the BMOs extending repeatedly beyond the MUC, rather than due to the maximization of the CO-surface interactions. The AO components, however, describe the delocalized aspect of the chemisorptive interactions, and may affect the adsorption of the second molecules to be adsorbed.

The calculated results are compared with some experimental data. Adsorbed CO easily dissociates on the W(110) surface [3–5]. The remarkable weakening of the CO bond is observed on the stepped Pt surfaces [6, 7], though the fission of the bond seems to require the kinked structure [8]. So it is instructive to discuss the similarity and difference between the interactions on the W(110) surface and at the bottom site on the Pt(112) surface. The σ donation is enhanced in these two systems compared with the other systems. The σ donation is, however, not effective for the fission of C—O bond as understood from the pattern of the CO region in the ILO-1 shown in Figs. 2 and 3. Actually, the explanation for increased weakening of the bond in the two systems is found in the enhanced π type interactions. In the W(110)+CO system, the π back donation represented by the ILO-2 contributes most effectively to the bond fission, but the π donation represented by the ILOs-1 and -2, which mixes with the σ donation, is more important at the bottom site on the Pt(112) surface. Thus, the mechanism of C—O bond fission is different in the two systems at least in the initial steps, though the increased weakening of C—O bond obtained in the calculation is consistent with the corresponding experimental data.

Finally, the criteria for the construction of the ILO are compared between the present and the previous articles [1]. The ILO is determined so that the CT interactions between subsystem MOs may become extremum in the present article. This criterion will be most favorable to discuss new bond formation and old bond fission if the atomic configuration within each subsystem is not so distant from its equilibrium configuration. As the reaction proceeds, however, the change in the configuration of subsystems becomes large, and the distinction between the occupied and vacant subsystem MOs becomes less valid. In this case, the criterion described in the previous article seems more suitable, where all the interactions between subsystems are adopted to determine the ILO.

5. Conclusion

In this article, we presented a new method to investigate the quantum chemical interactions between subsystems which constitute a reaction system. In this method new orbitals (the ILOs) are constructed from canonical MOs of the system so that the magnitude of CT interactions between the subsystems may become maximum or minimum in the representation by the ILO. In other words, the interactions are localized upon a few ILOs, and the number of orbitals responsible for the interactions remarkably decreases, whereas the interactions spread out over many MOs. So the ILO is an orbital which extracts the modes of interaction from the MOs for the system. This advantage makes it possible to comprehend complex interactions in large systems in terms of the orbital

interaction as well as simple interactions in small systems. Actually, the modes of interaction are clearly visualized by illustrating the orbital patterns for a few ILOs corresponding to the maximized interaction. The method was applied to the investigation of the adsorbate-surface interactions in the four chemisorption systems; Pt(111)+CO, W(110)+CO and Pt(112)+CO (terrace and bottom sites). The interactions in all the systems were understood in terms of the σ and π donation and the π back donation, while the σ and π donations remarkably mix with each other at the bottom site on the Pt(112) surface. Not only the 5σ orbital but also the 3σ and 4σ orbitals on CO participate in the σ donation. The π back donation and the π donation are important for the increased C—O bond weakening in the W(110)+CO and Pt (112)+CO (bottom site) systems, respectively. The present calculation was carried out using the CNDO/2 approximation, but the method is also applicable to *ab initio* calculations based on a single determinant wave function.

Acknowledgement. The authors thank Professor K. Fukui and Professor H. Kato for their helpful advice and discussion. The Data Processing Center of Kyoto University is acknowledged for generous use of the FACOM M200 computer.

References

1. Kobayashi, H., Yoshida, S., Kato, H., Yamaguchi, M.: see this Volume
2. For a review, Castner, D. G., Somorjai, G. A.: Chem. Rev. **79**, 233 (1977), see also Brodén, G., Rhodin, T. N., Brucker, G., Benbow, R., Hurych, Z.: Surface Sci. **59**, 593 (1976)
3. Bradshaw, A. M., Menzel, D., Steinkilberg, M.: Chem. Phys. Lett. **28**, 516 (1974)
4. Backx, C., Willis, R. F., Feuerbacher, B., Fitton, B.: Surface Sci. **68**, 516 (1977)
5. Chen, J.-R., Gomer, R.: Surface Sci. **81**, 589 (1979)
6. Collins, D. M., Spicer, W. E.: Surface Sci. **69**, 85, 114 (1977)
7. Netzer, F. P., Wille, R. A.: Surface Sci. **74**, 547 (1978).
8. Iwasawa, Y., Mason, R., Textor, M., Somorjai, G. A.: Chem. Phys. Lett. **44**, 468 (1976)
9. Brodén, G., Pirug, G., Bonzel, H. P.: Chem. Phys. Lett. **51**, 250 (1977).
10. Plummer, E. W., Salaneck, W. R., Miller, J. S.: Phys. Rev. **B18**, 1673 (1978).
11. Prasad, P. L., Singh, S.: J. Chem. Phys. **67**, 4384 (1977)
12. Rosén, A.: Grundevik, P., Morović, T.: Surface Sci. **95**, 477 (1980)
13. For a review, Pople, J. A., Beveridge, D. L.: Approximate molecular orbital theory. New York: McGraw-Hill 1970
14. Clementi, E., Raimondi, D. L., Reinhardt, W. P.: J. Chem. Phys. **47**, 1300 (1967)
15. Burns, G.: J. Chem. Phys. **41**, 1521 (1964).

Received February 15, 1982